Mechanistic Investigation on Salt-Mediated Formation of Free-Standing Co_3O_4 Nanocubes at 95 °C

Rong Xu and Hua Chun Zeng*

Department of Chemical and Environmental Engineering, Faculty of Engineering, and Chemical and Process Engineering Centre, National University of Singapore, 10 Kent Ridge Crescent, Singapore 119260

Received: May 1, 2002; In Final Form: November 11, 2002

The transformation process of various cobalt hydroxide and hydroxide nitrate into final free-standing Co_3O_4 nanocubes with a uniform size of ca. 47 nm has been investigated with X-ray diffraction (XRD), scanning electron microscopy (SEM), Fourier transform infrared spectroscopy (FTIR), thermogravimetric analysis (TGA), and high-resolution transmission electron microscopy (HRTEM) methods. It is found that during their sequential oxidation under air bubbling at 95 °C, β-$Co(OH)_2$ and $Co^{II}(OH)_{2-x}(NO_3)_x{\cdot}nH_2O$ solid phases are gradually oxidized to a mixture of $Co^{II}_{1-x}Co^{III}_x(OH)_2(NO_3)_x{\cdot}nH_2O$ and Co_3O_4 in high concentration nitrate salt (e.g., $NaNO_3$) solution, through which the single-phase Co_3O_4 nanocubes have been formed with a prolonged oxidation. With the mediation of $NaNO_3$ salt in synthesis, formation of perfectly faceted Co_3O_4 nanocubes can be attributed to a lowering in O_2 solubility and creation of salt−$(solvent)_n$ diffusion boundary on the surfaces, which retards the cobalt oxidation and alters the normal interfacial growth under nonsalted conditions.

Introduction

Over the past decade, synthesis of zero- and one-dimensional (0D and 1D) materials has gained considerable interest in development of new generation optical, electronic, magnetic, and catalytic materials.[1−10] In particular, 1D tubular and rodlike materials such as elemental carbon, metals, semiconductor alloys, sulfides, oxides, and hydroxides have been investigated extensively.[1−4] Zero-dimensional dotlike materials (quantum dots) such as metal and semiconductors, on the other hand, are normally prepared into spherical nanoparticles with the assistance of solvents or surfactants or both for further stabilization and assembly processing.[5−10] To realize their optical, magnetic, and electrical properties of size-quantized state of matter, monodispersed particles with 0D are highly desirable.[5−10] Regarding the synthesis of ceramic nanoparticles, major research effort has been devoted to increase dispersibility of pristine materials because permanent aggregation of nanoparticles often occurs during thermal treatments at elevated temperatures. For example, the synthesis of free-standing lead zirconate titanate (a ferroelectric) nanoparticles has been successful with a modified sol−gel method at low temperatures.[11] Spinel Co_3O_4 is an important magnetic *p*-type semiconductor that has been widely used as solid-state sensors, ceramic pigments, intercalation compounds for energy storage, rotatable magnets, heterogeneous catalysts, and electrochromic devices.[12−16] Although monodispersed Co_3O_4 crystallites (ca. 100 nm) had been synthesized some 23 years ago with a "forced hydrolysis" method at relatively low temperatures,[13,14] the actual formation process has still remained largely unknown.

Very recently, we have experimentally elucidated a growth mechanism for the 1D β-$Co(OH)_2$ nanorods via ethylenediamine-mediated synthesis.[15] In this paper, as a preliminary effort in understanding the formation process of 0D cobalt spinel, we will report a mechanistic investigation on salt−solvent synthesis of Co_3O_4 nanocrystallites. Individual Co_3O_4 crystallites in almost perfect cubic shape with a uniform size of around 47 nm can be generated sequentially from three precursor compounds under air atmosphere in aqueous solution at a temperature as low as 95 °C. By adding $NaNO_3$ salt, the observed facet growth in these free-standing nanocubes can be explained with a lowering in O_2 solubility and presence of a salt−$(solvent)_n$ diffusion boundary on the surfaces of Co_3O_4, which retards the cobalt oxidation and interfacial growth.

Experimental Section

Nanocubes of spinel oxide Co_3O_4 were prepared with a nitrate-salt-mediated synthesis at 95 °C in aqueous solution. Twenty milliliters of 1.0 M cobalt nitrate solution ($Co(NO_3)_2{\cdot}6H_2O$, >99%, Merck) was added into a three-necked round-bottom flask containing 100.0 mL of 0.3 M sodium hydroxide (NaOH, >98%, Fluka) solution and 90 g of sodium nitrate ($NaNO_3$, >99%, Nacalai Tesque) within 1 min, which resulted in an instantaneous precipitation. The flask was mounted with a water-cooled reflux unit, and the reaction system was bubbled with purified air (Messer) through the solution at 50 mL/min. Throughout the course of reaction (precipitation and aging), the solid−solution mixture was stirred vigorously at constant temperature, 95 °C. After a desired reaction time (1.5−96 h), the solid product was filtered and washed thoroughly with deionized water, followed by a vacuum-drying at room temperature overnight (sample series A). The solution after reactions was slightly acidic, and the pH value decreased gradually upon the aging time (e.g., 1.5 h, pH 5.9; 3 h, pH 5.9; 18 h, pH 4.6; 24 h, pH 4.3; 48 h, pH 3.2; 74 h, pH 3.2; measured with a pH meter at room temperature). Samples without addition of sodium nitrate in the alkaline solutions were also prepared, while the rest of the experimental conditions were kept the same (sample series B, reaction time 1.5−24 h). The as-prepared samples were investigated with X-ray diffraction (XRD, Shimadzu XRD-6000, Cu Kα radiation, $\lambda = 1.5406$ Å), Fourier transform infrared spectroscopy (FTIR, Shimadzu, FTIR-8108), and thermogravi-

* To whom correspondence should be addressed.Tel: +65 874 2896. Telefax: +65 779 1936. E-mail: chezhc@nus.edu.sg.

10.1021/jp021094x CCC: $25.00
Published on Web 01/01/2003

metric analysis (TGA) in a pure nitrogen flow (60 mL/min; Bio-Rad, TGA 2050, heating rate 10 °C/min). Morphology of the as-prepared samples was examined with scanning electron microscopy (SEM, JSM-5600LV). Free-standing Co_3O_4 nanocubes were prepared by a sonication method in which 3 mg of the as-prepared sample was suspended in 1 mL of acetone liquid in an ultrasonic water bath for 40 min. A drop of this suspension was placed onto a carbon-coated 200-mesh copper grid and then dried at room temperature for a further investigation with transmission electron microscopy (TEM, JEM-2010, 200 kV).

Results and Discussion

Figure 1 shows an evolution of XRD patterns from the starting precursor precipitate to final cubic spinel oxide, Co_3O_4. After 1.5 h aging, the precipitate was a mixture of β-phase cobalt hydroxide, β-$Co(OH)_2$ (brucite-like structure),[17] and cobalt hydroxide nitrate, $Co^{II}(OH)_{2-x}(NO_3)_x \cdot nH_2O$ ($x \approx 0.2-0.5$, $n \approx 0.1$; also a layered compound)[17] in which nitrate anions had been intercalated into interlayer space of the brucite-like sheets with one oxygen atom directly attached to a metal cation.[17] The formation of $Co^{II}(OH)_{2-x}(NO_3)_x \cdot nH_2O$ compound, which was not formed in all of our previous investigations,[18] is due to a high concentration of nitrate anions introduced in the synthesis and thus a strong competition between the nitrate anions (largely from $NaNO_3$ salt added) and hydroxide ions to chelate to divalent cobalt during the rapid precipitation. It had been further proven that without adding $NaNO_3$ salt, β-$Co(OH)_2$ was the only product phase under the same synthetic conditions (1.5 h, will be presented herein). With a longer reaction time in mother liquor, two more solid phases were generated with air within the starting mixture. The first one, $Co^{II}_{1-x}Co^{III}_x(OH)_2(NO_3)_x \cdot nH_2O$ (a hydrotalcite-like compound, in which cobalt ions have mixed +2 and +3 oxidation states), was formed owing to an oxygen oxidation of divalent cobalt into the trivalent, the structure and composition of which had been determined in our previous investigation ($x \approx 0.26-0.28$, $n \approx 0.3-0.6$).[18] Note that the structural details of $Co^{II}(OH)_{2-x}(NO_3)_x \cdot nH_2O$ and $Co^{II}_{1-x}Co^{III}_x(OH)_2(NO_3)_x \cdot nH_2O$ are substantially different and their characteristic XRD patterns have been well documented (see also Figure 1).[17,18] The second one is cubic-phase Co_3O_4 spinel, the end product of the present study, starting to form at a reaction time of 10 h. The $Co^{II}(OH)_{2-x}(NO_3)_x \cdot nH_2O$ phase disappeared completely over an aging period of 18−21 h, and the remaining phases were $Co^{II}_{1-x}Co^{III}_x(OH)_2(NO_3)_x \cdot nH_2O$ and final product Co_3O_4. The single phase of cubic-phase Co_3O_4 spinel could be obtained with longer reaction times (>24 h) at 95 °C.

The formation of Co_3O_4 spinel in these samples is also confirmed with their two fingerprint IR absorptions at 667−669 and 584−587 cm^{-1}. To quantify their thermal properties and phase composition, the precipitate products at different reaction stages were characterized with TGA under nitrogen atmosphere. In all samples, except for those reacted for more than 24 h, there is only a major weight loss at 181−209 °C that can be assigned to an overall thermal decomposition of colbalt(II) hydroxide, cobalt(II) hydroxide nitrate and cobalt(II)−cobalt(III) hydrotalcite-like phases (Figure 1), noting that the percentage of loss is proportional to the remained nonspinel phases. In sample A24, for example, the weight loss at 183 °C is only about 6%. Because of a lack of weight loss for sample of A36, it is concluded that this sample had been in a single-phase Co_3O_4 prior to TGA measurement, as revealed by XRD study in Figure 1. Over 210−600 °C, there is no any further weight loss for all of the samples, which indicates that the thermally decomposed products had been largely in cobalt oxide forms (CoO and Co_3O_4) before 210 °C.

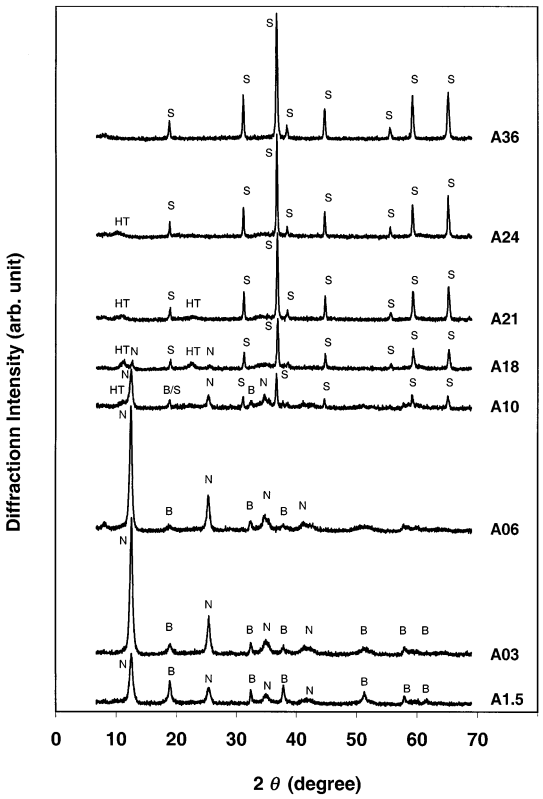

Figure 1. XRD pattern evolution for the A series precipitates after 1.5−36 h (i.e., samples A1.5 to A36) reactions at 95 °C: B = β-$Co(OH)_2$; N = $Co^{II}(OH)_{2-x}(NO_3)_x \cdot nH_2O$; HT = $Co^{II}_{1-x}Co^{III}_x(OH)_2(NO_3)_x \cdot nH_2O$; S = Co_3O_4 phase.

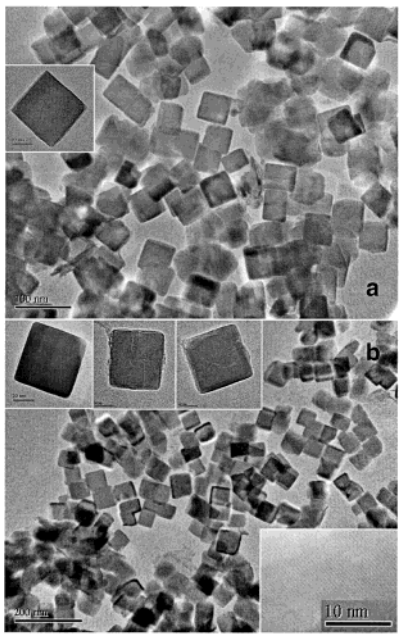

Figure 2. TEM images with different magnifications for the Co_3O_4 nanocubes formed after reactions at 95 °C for (a) 35 and (b) 48 h with $NaNO_3$. The lower-right insert shows the lattice fringes with interplanar distance d_{111}.

Overall crystallite morphologies of the as-prepared samples were first examined with SEM. In agreement with the XRD results, layered features of β-$Co(OH)_2$ and $Co^{II}(OH)_{2-x}(NO_3)_x \cdot nH_2O$ can be seen in the platelet-like morphology in the samples with a short aging (e.g., 6 h), while the solid aggregates of Co_3O_4

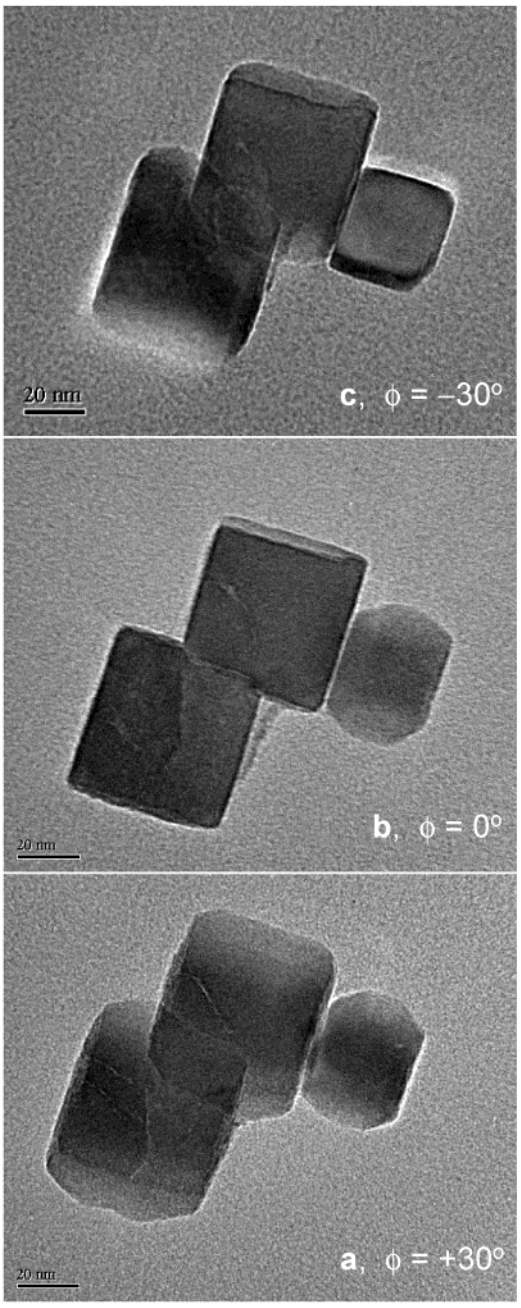

Figure 3. TEM confirmation of cubic morphology with different tilted angles (ϕ) for the Co_3O_4 nanocubes formed after 48 h reactions at 95 °C with $NaNO_3$.

give no preferential orientation for the growth or packing in the samples after a long aging (e.g., 36 h) because of cubic symmetry of the spinel. Owing to low-temperature synthesis, the crystallites can be easily dispersed into individual ones with a sonication treatment at room temperature in acetone solvent (see Experimental Section). Some representative TEM images of these dispersed Co_3O_4 nanocubes (95°C, 35 and 48 h) are shown in Figure 2. As can be seen, all crystallites are faceted with six low Miller-index planes of {100}, {010}, and {001}. Most of them are sitting along the [001] axis, giving rise to an overall squarely cubic morphology. Some apparently elongated crystallites (rectangular) are also perfect cubes; they are in fact seen along their [110] axis (instead of the common [001] axis), which is confirmed in Figure 3 in our tilted-angle TEM experiment. The Co_3O_4 nanocubes are well crystallized, showing a sharply resolved interplanar spacing of $d_{111} = 4.6 \pm 0.2$ Å[19]

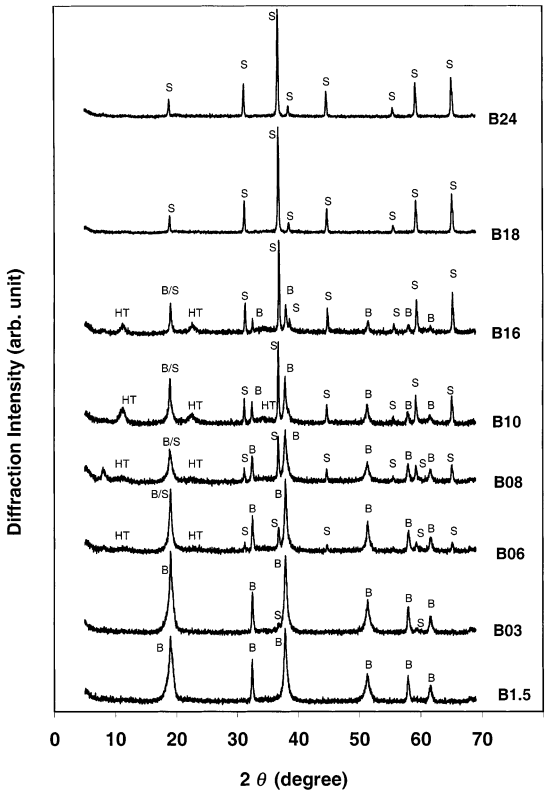

Figure 4. XRD pattern evolution for the B-series precipitates after 1.5−24 h (i.e., samples B1.5 to B24) reactions at 95 °C without using $NaNO_3$: B = β-$Co(OH)_2$; HT = $Co^{II}_{1-x}Co^{III}_x(OH)_2(NO_3)_x \cdot nH_2O$; S = Co_3O_4 phase.

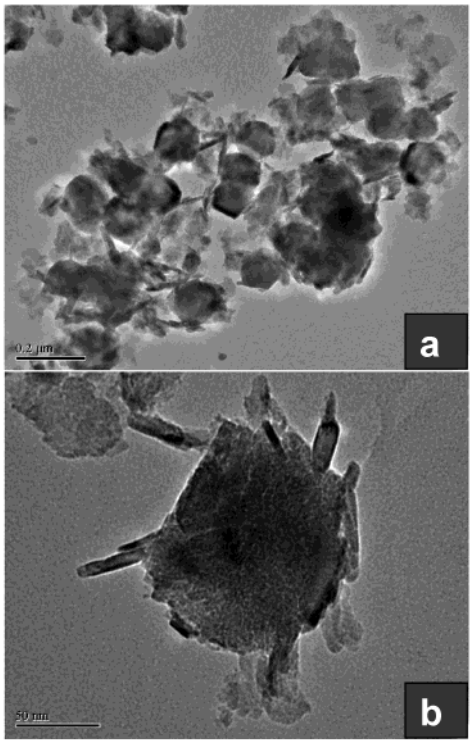

Figure 5. TEM images with different magnifications (a and b) for the Co_3O_4 crystallites formed after reactions at 95 °C for 24 h (sample B24) without using $NaNO_3$.

in TEM images (insert, Figure 2b) with higher resolutions for some [111]-standing crystallites, and they are clearly free-standing, although most of them are loosely aligned, probably through their little magnet dipoles. The average size of these

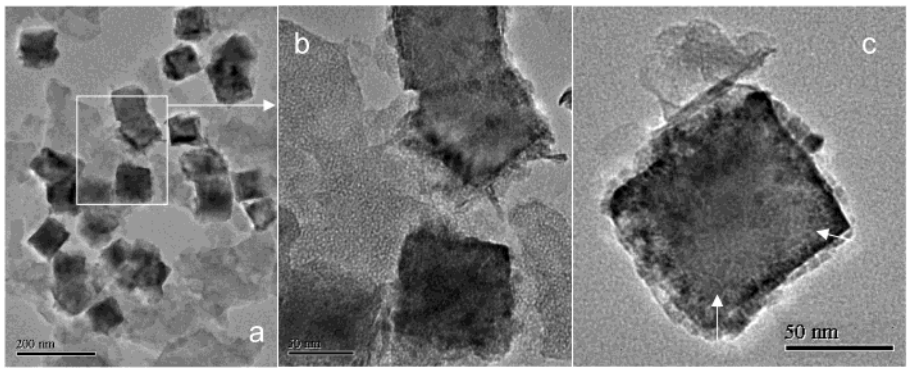

Figure 6. A reaction intermediate mixture of $Co^{II}_{1-x}Co^{III}_x(OH)_2(NO_3)_x{\cdot}nH_2O$ and Co_3O_4 nanocubes (TEM images for the sample after 21 h reactions at 95 °C with $NaNO_3$): (a) precipitate mixture; (b) an enlarged part in panel a; (c) Co_3O_4 nanocube crystal interface. The interface is indicated with arrows.

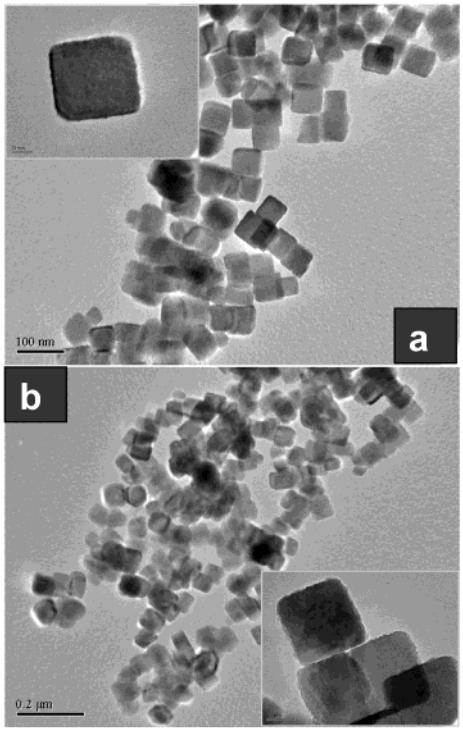

Figure 7. TEM images with different magnifications for the Co_3O_4 nanocubes formed after reactions at 95 °C for (a) 78 and (b) 96 h with $NaNO_3$.

tiny cubes (Figure 2) is about 47 nm (with a small population standard deviation $\sigma = 7.56$), noting that they are as-prepared without any additional size screening. Based on our powder XRD analysis, the unit cell constant in cubic symmetry for these nanocubes is $a = 8.09 \pm 0.01$ Å, which is in excellent agreement with the reported literature.[19] Other crystallite sizes of Co_3O_4 nanocubes ranging from 10 to 100 nm can also be achieved by varying synthetic conditions such as reaction temperature and concentrations.[20]

As reported in Figure 4 for sample series B, without adding $NaNO_3$ salt into the synthesis while keeping other synthetic parameters unchanged, the intermediate compound of cobalt hydroxide nitrate, $Co^{II}(OH)_{2-x}(NO_3)_x{\cdot}nH_2O$,[17] was skipped, and the initial β-$Co(OH)_2$ started to be converted to Co_3O_4 spinel (after 3 h, B3) and to $Co^{II}_{1-x}Co^{III}_x(OH)_2(NO_3)_x{\cdot}nH_2O$ (after 6 h, B6); the latter compound was then transformed totally to Co_3O_4 spinel with prolonged reactions. Single-phase spherelike (instead of perfect cubic morphology in sample series A) Co_3O_4 crystallites ranging from 100 to 150 nm could be obtained with this route in a shorter reaction time of just 24 h, as shown in Figure 5a, compared to 35−48 h with the usage of sodium nitrate (47 nm, Figure 2). In particular, rodlike crystallites are randomly extruding from the large Co_3O_4 spheres (Figure 5b). Apparently, the $NaNO_3$ salt played a central role in changing the structure and chemical composition of precursor compounds, which leads to different reaction paths and rates to the final Co_3O_4. The solubility of oxygen in aqueous solution was greatly reduced owing to a high concentration of sodium nitrate in the mother liquor and its related salting-out effect.[21−23] A slower oxidation process is thus expected. Apart from the reduction in O_2 solubility, the ionic strength of the solution was increased greatly with the addition of sodium nitrate salt. The ionic strengths calculated for the starting alkaline solutions with and without 90 g of sodium nitrate are 10.9 and 0.3 M, respectively, using the equation given by Lewis and Randall.[24] The effect of this parameter on the properties of the final products will be further discussed herein.

A conversion intermediate phase is illustrated in Figure 6. After 21 h of the reactions (series A, see also Figure 1), the hydrotalcite-like compound $Co^{II}_{1-x}Co^{III}_x(OH)_2\ (NO_3)_x{\cdot}nH_2O$ (sheetlike layers, lighter; Figure 6a,b) still coexisted with Co_3O_4 nanocubes in the solid mixture. Different from the flat morphology shown in Figures 2 and 3, surfaces of these intermediate nanocubes are more irregular and less compact. In particular, the sharp interfaces between single-crystalline Co_3O_4 nanocubes (central part) and growing zone (outer part) can be clearly distinguished (Figure 6c). With a longer reaction time of 35−48 h, the inner growth interfaces are no longer observed, because they have been turned (or surfaced) into much smoother {100}, {010}, and {001} crystallographic planes (Figures 2 and 3). The straight growth interfaces and perfect cubic morphology of the final nanocrystals suggest that some small growth entities (such as atomistic species or cluster building blocks) should be responsible for this interfacial growth. Compared to the "forced hydrolysis" method, in which most of metal ions are still in aqueous phase after the precipitation under neutral or slightly acidic condition,[13,14] better utilization of metal source is achieved in our current synthesis because we are able to convert the majority of cobalt ions into various solid precursors under basic condition prior to their conversion to the final Co_3O_4 nanocubes.

In view of the smaller crystallites obtained in the sample series of A, it is believed that the high ionic strength has also played an important role in control of the particle sizes and morphologies. Interfacial tension has been lowered because of the screening of the interface with the electrostatic repulsion by increase of the surface charge density.[25,26] Under such conditions, extending the surface resulting in smaller particles involves no energetic penalty, which allows the formation of dimension-

ally stable particles.[25,26] In fact, the higher the ionic strength is, the smaller the particle size is.[27] This effect is further supported by the evidence of the similar crystallite sizes (ca. 45−50 nm) of the spinel Co_3O_4 at the reaction time span of 24−96 h, during which the ionic strength remained essentially the same. As demonstrated in Figure 7, prolonged reactions do not increase the size of Co_3O_4 nanocubes but increase the surface roughness owing to mechanical collisions among the crystallites under the prolonged stirring (see Experimental Section). Alternatively, the function of $NaNO_3$ salt can be considered as the creation of a diffusion barrier for the nanocube growth. In particular, the salt−(solvent)$_n$ clusters attracted on the surfaces of Co_3O_4 nanocubes might serve as a diffusion boundary layer to slow the decomposition of layered compound(s) and the subsequent Co_3O_4 interfacial growth, which seemed to be an important cause for the observed faceted growth and small-sized cubes.[28] Further investigations with other soluble inorganic salts including a variation of cation and anion species will be undertaken.

Conclusion

In summary, free-standing Co_3O_4 nanocubes with a uniform size of ca. 47 nm can be synthesized via designing precursor compounds and their subsequent oxidation conversion under high ionic strength conditions (by adding $NaNO_3$ salt in synthesis) at 95 °C. In aqueous solution, β-$Co(OH)_2$ and $Co^{II}(OH)_{2-x}(NO_3)_x \cdot nH_2O$ are gradually oxidized to $Co^{II}_{1-x}Co^{III}_x(OH)_2(NO_3)_x \cdot nH_2O$ and Co_3O_4 through which the final single-phase Co_3O_4 nanocubes can be prepared with a prolonged oxidation. Compared to the nonsalted conditions in sample series B, formation of faceted nanocubes in the series A can be attributed to a lowering in O_2 solubility and creation of salt−(solvent)$_n$ diffusion boundary, which retards the cobalt oxidation and interfacial growth. This investigation may provide general synthetic concepts for the synthesis of other nanosized metal oxides through design of precursor intermediates, including selection of related inorganic−organic salts and solvents under atmospheric or other high-pressure hydrothermal reaction conditions.

Acknowledgment. The authors gratefully acknowledge research funding (Grants R-279-000-064-112 and A/C50384) cosupported by the Ministry of Education and the National Science and Technology Board, Singapore.

References and Notes

(1) (a) Iijima, S. *Nature* **1991**, *354*, 56. (b) Ebbesen, T. W.; Ajayan, P. M. *Nature* **1992**, *358*, 220. (c) Peng, X.; Manna, L.; Yang, W.; Wickham, J.; Scher, E.; Kadavanich, A.; Alivisato, A. P. *Nature* **2000**, *404*, 59. (d) Gudiksen, M. S.; Wang, J.; Lieber, C. M. *J. Phys. Chem. B* **2001**, *105*, 4062. (e) Wu, Y.; Yang, P. *J. Am. Chem. Soc*. **2001**, *123*, 3165. (f) Tenne, R.; Margulis, L.; Genut, M.; Hodes, G. *Nature* **1993**, *360*, 444. (g) Feldman, Y.; Wasserman, E.; Srolovitz, D. J.; Tenne, R. *Science* **1995**, *267*, 222.

(2) (a) Ajayan, P. M.; Stephan, O.; Redlich, P.; Colliex, C. *Nature* **1995**, *375*, 564. (b) Lakshmi, B. B.; Patrissi, C. J.; Martin, C. R. *Chem. Mater*. **1997**, *9*, 2544 and references therein. (c) Aggarwal, S.; Monga, A. P.; Perusse, S. R.; Ramesh, R.; Ballaaarotto, V.; Williams, E. D.; Chalamala, B. R.; Wei, Y.; Reuss, R. H. *Science* **2000**, *287*, 2235.

(3) (a) Huang, M. H.; Wu, Y. Y.; Feick, H.; Tran, N.; Weber, E.; Yang, P. D. *Adv. Mater*. **2001**, *13*, 113. (b) Huang, M. H.; Mao, S.; Feick, H.; Yan, H.; Wu, Y.; Kind, H.; Webber, E.; Russo, R.; Yang, P. *Science* **2001**, *292*, 1897.

(4) Li, Y.; Sui, M.; Ding, Y.; Zhang, G.; Zhuang, J.; Wang, C. *Adv. Mater*. **2000**, *12*, 818.

(5) (a) de la Fuente, J. M.; Barrientos, A. G.; Rojas, T. C.; Rojo, J.; Cañada, J.; Fernández, A.; Penadés, S. *Angew. Chem., Int. Ed*. **2001**, *40*, 2257. (b) Wang, R.; Yang, J.; Zheng, Z.; Carducci, M. D.; Jiao, J.; Seraphin, S. *Angew. Chem., Int. Ed*. **2001**, *40*, 549. (c) Kim, B.; Tripp, S. L.; Wei, A. *J. Am. Chem. Soc*. **2001**, *123*, 7955.

(6) (a) Black, C. T.; Murray, C. B.; Sandstrom, R. L.; Sun, S. *Science* **2000**, *290*, 1131. (b) Diehl, M. R.; Yu, J.-Y.; Heath, J. R.; Held, G. A.; Doyle, H.; Sun, S.; Murray, C. B. *J. Phys. Chem. B* **2001**, *105*, 7913.

(7) Chen, S. W.; Sommers, J. M. *J. Phys. Chem. B* **2001**, *105*, 8816.

(8) Canton, P.; Meneghini, C.; Riello, P.; Balerna, A.; Benedetti, A. *J. Phys. Chem. B* **2001**, *105*, 8088.

(9) Vaucher, S.; Li, M.; Mann, S. *Angew. Chem., Int. Ed.* **2000**, *39*, 1793.

(10) Mamedov, A. A.; Belov, A.; Giersig, M.; Madedova, N. N.; Kotov, N. A. *J. Am. Chem. Soc.* **2001**, *123*, 7738.

(11) Liu, C.; Zou, B.; Rondinone, A. J.; Zhang, Z. J. *J. Am. Chem. Soc.* **2001**, *123*, 4344.

(12) (a) Ocana, M.; Gozalez-Elipe, A. R. *Colloids Surf., A* **1999**, *157*, 315. (b) Barreca, D.; Massignan, C.; Daolio, S.; Fabrizio, M.; Piccirillo, C.; Armelao, L.; Tondello, E. *Chem. Mater*. **2001**, *13*, 588. (c) del Barco, E.; Asenjo, J.; Zhang, X. X.; Pieczynski, R.; Julia, A.; Tejada, J.; Ziolo, R. F.; Fiorani, D.; Testa, A. M. *Chem. Mater*. **2001**, *13*, 1487.

(13) Sugimoto, T.; Matijevic, E. *J. Inorg. Nucl. Chem*. **1979**, *41*, 165.

(14) Matijevic, E. *Chem. Mater*. **1993**, *5*, 412.

(15) Sampanthar, J. T.; Zeng, H. C. *J. Am. Chem. Soc.* **2002**, *124*, 6668.

(16) (a) Zeng, H. C.; Lin, J.; Tan, K. L. *J. Mater. Res*. **1995**, *10*, 3096. (b) Zeng, H. C.; Lim, Y. Y. *J. Mater. Res*. **2000**, *15*, 1250. (c) Ji, L.; Lin, J.; Zeng, H. C. *J. Phys. Chem. B* **2000**, *104*, 1783.

(17) (a) Rajamathi, M.; Kamath, P. V.; Seshadri, R. *Mater. Res. Bull*. **2000**, *35*, 271. (b) Rajamathi, M.; Thomas, G. S.; Kamath, P. V. *Proc. − Indian Acad. Sci., Chem. Sci.* **2001**, *113*, 671. (c) N. Zotov; Petrov, K.; Dimitrova-Pankova, M. *J. Phys. Chem. Solids* **1990**, *51*, 1199. (d) Effenberger, H. *Kristallografiya* **1983**, *165*, 127.

(18) (a) Xu, Z. P.; Zeng, H. C. *J. Mater. Chem*. **1998**, *8*, 2499. (b) Xu, Z. P.; Zeng, H. C. *Chem. Mater*. **1999**, *11*, 67. (c) Xu, Z. P.; Zeng, H. C. *Chem. Mater*. **2000**, *12*, 3459.

(19) Joint Committee on Powder Diffraction Standards, International Centre for Diffraction Data, Card No. 43-1003, Swarthmore, PA, 1996.

(20) Feng, J.; Zeng, H. C. *Chem. Mater*., submitted for publication.

(21) Elliot, A. J.; Chenier, M. P.; Ouellette, D. C. *Fusion Eng. Des.* **1990**, *13*, 29.

(22) Schumpe, A. *Chem. Eng. Sci.* **1993**, *48*, 153.

(23) Tan, Z. Q.; Gao, G. H.; Yu, Y. X.; Gu, C. *Fluid Phase Equilib*. **2001**, *180*, 375.

(24) Snoeyink, V. L.; Jenkins, D. *Water Chemistry*, 1st ed.; John Wiley & Sons: New York, 1980; Chapter 3, p 75.

(25) Vayssieres, L.; Beermann, N.; Lindquist, S. E.; Hagfeldt, A. *Chem. Mater*. **2001**, *13*, 233.

(26) Jolivet, J. P.; Tronc, E.; Chaneac, C. *Eur. Phys. J.: Appl. Phys.* **2000**, *10*, 167.

(27) Vayssieres, L.; Chaneac, C.; Tronc, E.; Jolivet, J. P. *J. Colloid Interface Sci*. **1998**, *205*, 205.

(28) Dedonder-Lardeux, C.; Gregoire, G.; Jouvet, C.; Martrenchard, S.; Solgadi, D. *Chem. Rev.* **2000**, *100*, 4023.